



MSc Thesis

Prediction of polyadenylation motives with the help of 3' UTR secondary structure

Moritz Kiekeben

Matrikelnummer: 4179384

moritz.k@fu-berlin.de

Betreuer: Prof. Dr. Peter N. Robinson

Eingereicht bei:

Berlin, March 25, 2017

Abstract

Abstract

Declaration of authorship

I hereby declare that the thesis submitted is my own unaided work. All direct or indirect sources used are acknowledged as references.

I am aware that the thesis in digital form can be examined for the use of unauthorized aid and in order to determine whether the thesis as a whole or parts incorporated in it may be deemed as plagiarism. For the comparison of my work with existing sources I agree that it shall be entered in a database where it shall also remain after examination, to enable comparison with future theses submitted. Further rights of reproduction and usage, however, are not granted here.

This paper was not previously presented to another examination board and has not been published.

March 25, 2017

Moritz Kiekeben

Contents

1	Introduction	1
1.1	Motivation	1
1.2	Aim	1
1.3	Existing tools	1
1.4	Background	2
1.4.1	Polyadenylation	2
1.4.2	Alternative polyadenylation	3
1.4.3	Scientific history of polyadenylation	4
1.5	Messenger ribonucleic acid (mRNA)	4
1.5.1	3' UTR	5
1.6	RNA secondary structure prediction	6
1.6.1	Single sequence secondary structure prediction	7
1.6.2	Comparative secondary structure prediction	8
1.6.3	McCaskill algorithm - calculating BPPs	9
1.6.4	ViennaRNA	10
2	Material and Methods	11
2.1	Prediction of polyadenylation signals using fuzzy logic	11
2.2	Adding base pair probabilities to the PAS prediction	12
2.3	getting fucking annoyed with the bloody writing	12
2.4	Dataset	12
3	Results	13
3.1	Coole ergebnisse für coole Menschen	13
3.2	Resultate, die die Welt verändern werden. So Great!	13
4	Conclusion/Discussion	14

1 Introduction

1.1 Motivation

The polyadenylation signal (PAS) is part of the 3' untranslated region(UTR) of almost every messenger RNA (mRNA). It is the binding site for a protein complex that causes the formation of the polyadenylation tail(poly(A)-tail). This tail of adenosines prevents the degradation of the mRNA in the cytoplasm effectively affecting the half-life of a mRNA and thereby raising the chance to be translated into a protein by the ribosome. As such, variants that have an impact on the efficiency of the PAS are potentially pathogenic due to their interference with the gene expression. Chen et al. wrote a review about diseases caused by PAS-affecting mutations.

reference
needed

Prediction of polyadenylation sites has been attempted several times with moderate success in the last twenty years. Seeing that we cannot predict PASs with high accuracy prompts the question if we have enough knowledge about the structure of polyadenylation sites. Analyzing the secondary structure of the 3' UTR might give us more insight and allows the use of more characteristics for an accurate prediction.

reference
and
example
needed

Accurately identifying functional PASs enables us to detect disease-causing mutations easier or helps in gene prediction.

1.2 Aim

The aim is to analyze the effect of mRNA base pair probabilities (BPP) on the prediction accuracy of functional, human polyadenylation signals. If possible, we want to improve the prediction accuracy since we assume that a conserved secondary structure is necessary for the polyadenylation process to work. The BPPs should reflect this conserved secondary structure at the polyadenylation signal sites.

1.3 Existing tools

There is a large pool of available methods and programs to predict functional polyadenylation sites. The majority of them rely on machine learning algorithms like neural network [14], Hidden Markov Model [7, 8], linear discriminant function [16], quadratic discriminant function [19], Support Vector Machine [12, 3] or Random Forest [9]. But other options are also available, e.g. position weight matrix [11] and fuzzy logic [10].

The afore-mentioned methods and programs usually utilize the base composition surrounding the polyadenylation site to distinguish a functional PAS

from a non-functional one. Almost all programs achieve moderate prediction accuracies of 50% to 60%, leaving room for improvement. Since RNA secondary structure is becoming more and more the focus of scientific attention, incorporating features of secondary structure prediction might improve the accuracy to predict functional polyadenylation sites.

1.4 Background

1.4.1 Polyadenylation

Polyadenylation (poly(A)) takes place in the cell nucleus and describes the process of adding adenosines to the 3' end of precursor mRNA (pre-mRNA), i.e. messenger RNA that has been recently transcribed and has yet to undergo any post-transcription steps like splicing or polyadenylation. Most eukaryotic mRNAs have a polyadenylated tail, except for histone mRNAs.

After the transcription of the pre-mRNA by the RNA polymerase II the new transcript is cleaved and then polyadenylated. Cleavage is mediated by the enzyme complex cleavage and polyadenylation specificity factor (CPSF) which binds to the polyadenylation signal (PAS) sequence about 10 to 50 nucleotides upstream of the cleavage site. The canonical PAS motif in humans is AAUAAA but there exist at least ten variants which bind less potently to CPSF. The motif sequence is also dependent on the taxonomic group, e.g. fungi and humans have a different canonical PAS motif.

CPSF is usually assisted by two other protein complexes called cleavage stimulation factor (CstF) and cleavage factor I (CFI). CstF binds to a U/GU-rich region downstream of the cleavage site, the downstream sequence element (DSE), while CFI binds to a uracil-rich region upstream of the PAS, the upstream sequence element (USE). The presence of these two proteins greatly enhances the efficiency of the cleavage that occurs around 10 to 50 nucleotides downstream of the PAS.

After the cleavage CPSF recruits the poly(A) polymerase enzyme which is responsible for the addition of the adenosines at the cleavage site, resulting in the poly(A) tail. The length of the poly(A) tail is usually 200 to 250 adenosines long in mammals and differs in other taxonomic groups. Yeast, for example, only has a 80 nucleotides long poly(A) tail. The length of the tail is important for the survival of the mRNA, the shorter it is the more likely the mRNA is going to be degraded. Thus, the tail influences the half-life of a mRNA and with that the chance of the mRNA to be translated into a protein.

reference
needed,
use the
one
from
wiki
"polyadeny-
lation"

reference
needed

reference
needed

reference
needed

1.4.2 Alternative polyadenylation

The presence of multiple polyadenylation sites in one transcript is termed alternative polyadenylation (APA). It is a common occurrence with at least half of human transcripts exhibiting this phenomenon. [6] Messenger RNAs from the same transcript can have identical coding sequence (CDS) but varying 3' UTR lengths, although uncommon, the coding sequence can be affected by APA causing another protein to be translated.

reference
needed

Elkon et al. differentiate between four classes of APA: tandem 3'UTR APA, alternative terminal exon APA, intronic APA and internal exon APA (see Fig. 1) The most common class is tandem 3' UTR APA which is responsible for mRNAs with identical CDS but different 3' UTRs lengths, as described earlier. The other three APA classes will potentially create mRNAs with differing CDSs and are much rarer than tandem 3' UTR APA.

We can conclude that tandem 3' UTR is a mechanism to regulate the expression of a protein by altering the length of its corresponding mRNAs' 3'UTRs, which is a docking platform for various inhibitory factors like miRNAs. The other three classes, on the other hand, allow for more gene functionality since APA events are able to alter the CDS of mRNAs of one transcript and therefore, enable the translation of proteins with different functions.

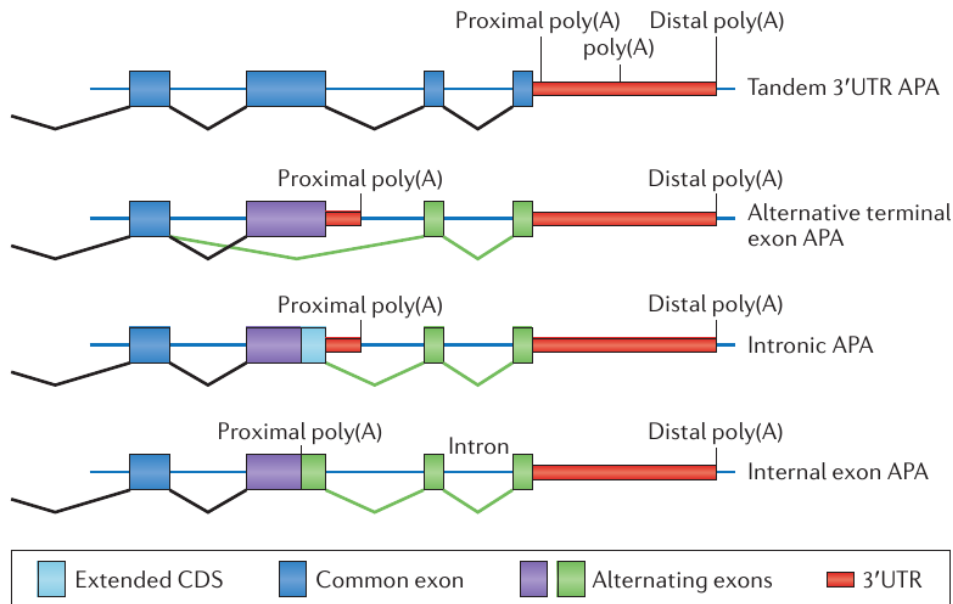


Figure 1: insert shitty text here

1.4.3 Scientific history of polyadenylation

The enzyme polyadenylate polymerase which catalyzes the polyadenylation reaction was first discovered in 1960. [4] But the protein's function was revealed about a decade later. [5] At that time it was still a mystery why most mRNAs have polyadenylated tails.

In the early 1980s the role of the poly(A)-tail was largely elucidated: nuclear export, translation and stability of the mature mRNA. (reviewed in [2]).

It took another decade to discover the two primary proteins that mediate the 3' end cleavage and polyadenylation, namely CPSF and CStF. The number of participating proteins has since increased and recent publications mention several dozen cis-acting and auxiliary proteins or polypeptides working together in a large complex. [6]

2008 it became clear that most genes have more than one polyadenylation site, resulting in transcripts with different lengths but identical coding sequence. [18] The new finding was termed alternative polyadenylation (APA). Since APA influences the length of the 3' untranslated Region (3' UTR), it is part of gene expression because the longer the 3' UTR the more binding sites for mRNA-repressive micro RNAs (miRNA) a transcript can have. [17]

1.5 Messenger ribonucleic acid (mRNA)

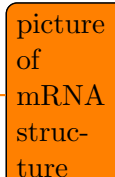
RNA is a molecule present in all lifeforms. There are many types of RNA like transfer RNA, ribosomal RNA, microRNA or messenger RNA. Most RNA types play key roles in coding (mRNA), decoding (tRNA), regulation (microRNA) and expression of genes.

mRNA is particularly interesting because it transports genetic information stored by the DNA to the protein synthesis factories of a cell, the ribosome. There, the mRNA specifies the amino acids sequence of a protein, making it an important component of the gene expression.

Every mRNA is composed of three parts: the 5' untranslated region (5' UTR), the coding sequence (CDS) and the 3' untranslated region (3' UTR).

The 5' UTR is described as the region upstream of the start codon. It contains structures to regulate the translation of the transcript, like the 5' guanine cap. Although, it is called UTR, the 5' UTR may contain upstream open reading frames translating to peptides that inhibit the translation of the CDS of the transcript.

The CDS contains the sequence that is translated into an amino acid polymer by the ribosome.



picture
of
mRNA
struc-
ture

The 3' UTR is defined as the region downstream of the stop codon. Because my thesis is focused on this region, it has a section of its own. (see 1.5.1)

Messenger RNA is generated by the RNA polymerase II protein during the transcription process of a protein-coding gene. While prokaryotic and archaeal mRNA are rarely modified, eukaryotic mRNA is usually subject to many processing steps, including the addition of a 5' cap, splicing and polyadenylation. To distinguish between nascent and processed mRNA, the literature has termed them precursor mRNA and mature mRNA correspondingly.

The 5' cap is a special guanine that is added co-transcriptionally to the 5' end of a mRNA. It is needed for the transport of the mRNA from the nucleus to the cytoplasm and prevents the degradation by exonucleases. The cap is also important for the initiation of the translation in the ribosome.

Splicing takes place during or after transcription and is responsible for the removal of the introns and the joining of the exons of most eukaryotic pre-mRNAs. Splicing can create different mRNAs and thus different proteins from the same pre-mRNA.

Polyadenylation occurs right after the cleavage of the transcript and describes the process of adding adenosines at the 3' end of the mRNA.

reference
needed

1.5.1 3' UTR

The three prime untranslated region is usually part of the terminal exon of a transcript and starts where the coding sequence ends. It can span over several exons but that is uncommon. The length of the 3' UTR is quite variable in humans and can range from 60 to 4000 nucleotides. However, the average size is about 800 nucleotides. Another often analyzed feature is the mean GC-content which is 45% for 3' UTRs of vertebrates. These characteristics differentiate the 3' UTR from the 5' UTR, which is on average only 200 nucleotides long and has a mean GC-content of about 60%.

Although the 3'UTR is not translated into a protein, it contains many regulatory elements and regions which affect the translation efficiency, localization and stability of the mRNA.

3' utr,
source
[3]

One of these regulatory elements are miRNA response elements (MREs). Micro RNAs are about 20 nucleotides long and usually have an inhibitory effect on mRNA by inducing degradation of the mRNA, thus affecting translation efficiency.

Like MREs, AU-rich elements (ARE) have a similar function. AREs are 50 to 150 nucleotides long and contain multiple copies of the sequence AUUUA. AREs can have inhibitory or enhancing effects but usually, like miRNA, they

reduce the probability of translation by inducing mRNA degradation.

The poly(A) tail is also part of the 3' UTR and is target of so-called poly(A) binding proteins (PABPs). PABPs are important for the translation, export and stability of an mRNA. They can also form a complex with proteins that bind to the 5' cap of the mRNA. The result is a circular mRNA which allows for easier translation initiation. While the presence of the poly(A) tail promotes translation, the absence of the tail usually leads to degradation by the exosome.

reference
needed

As we can see the 3' UTR is an important part of gene expression as it allows the cell to regulate the translation of proteins.

1.6 RNA secondary structure prediction

Recently transcribed RNA molecules fold themselves into their mature conformation by forming complementary base pairings. Where complementary base pairings are not possible, loops emerge. Therefore, we can group RNA secondary structures into two categories: base pair stacks and loops (see Fig.). Knowing this, we can model secondary structure of an RNA molecule using graph theory: Each nucleotide of an RNA secondary structure is a node in a labeled graph. Adjacent nucleotides and nucleotides forming base pairs are connected by edges. These base pair edges are subject to the following restrictions:

pic to
sec.
struc-
ture
types

1. only Watson-Crick or GU base pairs are allowed;
2. each node cannot have more than one base pair edge;
3. the distance on the phosphate backbone between two base pairs must be at least three nucleotides;
4. two base pair edges may not cross, i.e. if there is an edge $(i, j) \in G$ then there must not be an edge $(k, l) \in G$ with $i < k < j < l$.

The last restriction prohibits the formation of pseudoknots (see Fig.), a secondary structure that is difficult to predict. It has been shown that the pseudoknot problem is NP-complete, rendering a solution computationally very costly. [13]

definition
can
allow
edges
to cross
when k
| i and
 i | l j

Most types of RNA have a distinctive three-dimensional structure like the hairpin structure of miRNAs or the cloverleaf structure of tRNA. In general, the secondary structure is more conserved than the underlying nucleic acid sequence which, for example, is relevant for phylogenetics (evolutionary history of species) or medical studies, since mutations can alter the structure of an RNA molecule, potentially causing diseases.

pic with
sec.
struc-
tures

reference
needed

In-silico prediction of RNA conformation is an ongoing and complex research subject as experimental elucidation of RNA structure is still expensive and time-consuming. Nowadays we can predict the secondary structure reasonably well but tertiary and quaternary structure still remain difficult to predict accurately.

1.6.1 Single sequence secondary structure prediction

Experimental determination of molecule structure is often not feasible for the large amount of data DNA sequencers produce. For Bioinformaticians this usually means, that we need to predict the molecule structure given only its sequence. Predicting the exact spatial structure is difficult with the current state of research and usually we can retrieve relevant information just by looking at the secondary structures.

Zuker and Stiegler were one of the first to introduce a dynamic programming algorithm to solve the RNA folding problem. The Nussinov algorithm tries to maximize the number of base pairs, however this approach often led to inaccurate predictions.

A year later, Zuker and Stiegler published an algorithm that incorporates ideas from chemical thermodynamics to predict the most stable structure: the conformation of a mature molecule is most stable when its in the state of thermal equilibrium, i.e. in the state of minimum free energy (MFE). For RNA secondary structures the MFE is mainly determined by the sum of their hydrogen bonds and base stacks. The free energy values of base pair interactions and loops have been measured experimentally and are used in a nearest neighbor model by most implementations of the Zuker algorithm.

picture
maybe?

Zuker's algorithm uses two matrices $W(i, j)$ and $V(i, j)$. $W(i, j)$ denotes the minimum free energy of all structures that are formed by the subsequence i to j , while $V(i, j)$ denotes the minimum free energy of all structures that are formed by the subsequence i to j , if i and j are paired. The recursions for $W(i, j)$ are defined as follows:

$$W(i, j) = \min \begin{cases} W(i+1, j) \\ W(i, j-1) \\ V(i, j) \\ \min\{W(i, j) + W(k+1, j)\} \text{ where } i < k < j \end{cases}$$

The equation differentiates between four cases (top to bottom): i is unpaired, j is unpaired, i and j form a base pair and i and j form base pairs but not with each other. When i and j form a base pair we differentiate again between four cases by using the following equation:

$$V(i, j) = \min \begin{cases} eH(i, j) \\ eS(i, j) + v(i + 1, j - 1) \\ \min[eL(i, j, i', j') + V(i', j')] & \text{where } i < i' < j' < k \\ \min[W(i + 1, k) + W(k + 1, j - 1)] & \text{where } i + 1 < k < j - 1 \end{cases}$$

Here, eH calculates the energy of a hairpin loop spanning from i to j , eS is the energy of i and j being part of a base stack, the third case calculates the energy of a bulge or interior loop and the last case calculates the energy used for the formation of a multiloop.

The MFE of the whole sequence is then determined by $W(1, n)$ for a n nucleotides long sequence. The time complexity is $O(n^4)$ but can be improved to $O(n^3)$ by setting a limit to the maximum size of an interior loop (usually set to 30).

RNA secondary structure is usually more accurately predicted by the Zuker algorithm compared to the Nussinov algorithm. And although Zuker's approach is widely used nowadays there are a few issues:

- Pseudoknots cannot be detected by Zuker;
- The nearest neighbor model used to calculate the free energies is not precise enough;
- Some known RNAs do not fold themselves into their possible MFE structure;
- Some RNAs have more than one biologically active conformation.

While the pseudoknot problem is not efficiently solvable, the other three issues can be alleviated by taking a look at suboptimal structures, i.e. conformations that are equal or close to the MFE conformation. Many software packages allow the prediction of suboptimal structures.

1.6.2 Comparative secondary structure prediction

The basic idea behind comparative structure analysis is that important structural elements are usually highly conserved. Consequential, homologous sequences are likely to fold similarly. We want to extract information from the secondary structure conservation using multiple sequence alignments (MSAs). This means that we are not exactly predicting the secondary structures of a single molecule but a consensus secondary structure. There are three common methods available:

1.6.3 McCaskill algorithm - calculating BPPs

In 1990 [McCaskill](#) introduced an algorithm to compute the partition function of a single stranded nucleic acid sequence. The partition function is a method originating from mechanical statistics to calculate the likelihood of observing a certain state in a thermodynamic system. The states a system can adopt is called the ensemble. The partition function Q for the ensemble of all possible secondary structures S is defined as follows[15]:

$$Q = \sum_S e^{-\frac{F(S)}{k_B T}}$$

where

T = temperature in Kelvin

$F(S)$ = sum of the free energies of all loops of a secondary structure

k_B = Boltzmann constant

Thus, the total free energy of a secondary structure is assumed to be the sum of the free energies of its loops, as denoted by $F(S)$. Analogous to the Zuker algorithm, McCaskill uses a dynamic programming decomposition of the RNA folding problem to calculate the partition function. The recursive calculation of the partition function $Q(i, j)$ of a sequence interval $[i, j]$ looks like this[1]:

$$Q(i, j) = \overbrace{Q(i+1, j)}^{\text{i is unpaired}} + \overbrace{\sum_{i < k \leq j} Q^B(i, k) Q(k+1, j)}^{\text{i is paired}}$$

$Q^B(i, j)$ is defined as the partition function when i and j form a base pair. In that case, we differentiate between three additional cases:

$$Q^B(i, j) = \overbrace{\mathcal{H}(i, j)}^{\text{Hairpin}} + \overbrace{\sum_{i < k < l < j} \mathcal{J}(ij, kl) Q^B(k, l)}^{\text{Interior loop}} + \overbrace{Q^M(i+1, u) Q^{M1}(u+1, j-1) a(i, j)}^{\text{Multi loop}}$$

where

$$\mathcal{H}(i, j) = e^{-\frac{E_{\text{hairpin}}}{k_B T}}, \text{ Boltzmann factor of hairpin loop closed by } (i, j)$$

$$\mathcal{J}(ij, kl) = e^{-\frac{E_{\text{interior}}}{k_B T}}, \text{ B. factor of interior loop enclosed by } (i, j) \text{ and } (k, l)$$

$$a(i, j) = \text{Boltzmann weighted contribution to close a multi loop}$$

$Q^M(i, j)$ and $Q^{M1}(i, j)$ denote the partition functions for the multi loop contributions:

$$Q^M(i, j) = Q^M(i, j-1)c + \sum_{i < u < j} (Q^M(i+1, u) + c^{u-i})Q^B(u+1, j-1)b$$

$$Q^{M1}(i, j) = Q^{M1}(i, j-1)c + Q^B(i, j)b$$

The factors b and c are the Boltzmann weighted contributions of adding a base pair or an unpaired base to the multi loop, respectively.

With the help of the partition function we can now calculate the probability $p(i, j)$ of a base pair (i, j) forming in the ensemble, which is the quotient between the partition function $Q^{bp}(i, j)$ of all states that form the base pair (i, j) and the total partition function:

$$p(i, j) = \frac{Q^{bp}(i, j)}{Q(1, n)}$$

1.6.4 ViennaRNA

The Vienna RNA Package is a widely used library for RNA folding written in the programming language C. The first version was released in 1994 and offered the calculation of the MFE structure or the partition function. The package is shipped with several standalone CLI programs like RNAfold or RNAalifold.

den
rest aus
paper
[1] in
den ap-
pendix
um Q^{bp}
auszurech-
nen

reference
needed

2 Material and Methods

2.1 Prediction of polyadenylation signals using fuzzy logic

As mentioned in the introduction there are many methods available to predict polyadenylation signals. Kamasawa and Horiuchi introduced a method for detecting PASes using fuzzy logic. In contrast to boolean logic where a truth value can either be zero or one, truth values in fuzzy logic can be any real number in the range $[0, 1]$. Fuzzy logic is rather new in the fields of bioinformatics but has been employed to predict peptides binding to the major histocompatibility complex, data clustering, prognostication of cancer and prediction of genetic network .

Kamasawa and Horiuchi presented two programs in their original paper, "PolyFd" and "PolyFud". The difference between both programs is, that "PolyFd" is only evaluating the DSE of a PAS while "PolyFud" is evaluating the DSE and the USE. The method we will describe and implemented is based on "PolyFud", as it has been shown to be more accurate.

We will define two (membership) functions to determine the truth value of the DSE and the USE of a PAS:

$$tv_{DSE}(c_{uracil}, d) = \begin{cases} 1 & , 25 \leq d \leq 35 \\ m_1 c_{uracil} + b_1 & , 10 \leq d < 25 \\ m_2 c_{uracil} + b_2 & , 35 < d \leq 55 \\ 0 & , 10 > d > 55 \end{cases}$$

$$tv_{USE}(c_{uracil}) = \begin{cases} 1 & , c_{uracil} \geq 0.80 \\ m c_{uracil} + b & , 0.80 > c_{uracil} \geq 0.33 \\ 0 & , c_{uracil} < 0.33 \end{cases}$$

where

c_{uracil} = uracil content in a specific window

d = distance from the PAS

m = slope of the straight line equation

b = intercept of the straight line equation

reference
needed

reference
needed

reference
needed

reference
needed

2.2 Adding base pair probabilities to the PAS prediction

2.3 getting fucking annoyed with the bloody writing

2.4 Dataset

To analyze the sensitivity of the program, known PASes were collected from mRNA data provided by the Reference Sequence (RefSeq) database¹ to create a positive dataset. We only considered verified mRNA sequences (accession number prefix: NM_) with PAS motives that were listed in [Kamasawa and Horiuchi](#). This way, we obtained 6341 PASes with the following motif distribution:

motif	count
AATAAA	4972
ATTAAA	1276
TATAAA	20
AATATA	16
AGTAAA	11
AATGAA	10
AAGAAA	10
GATAAA	7
CATAAA	7
ACTAAA	6
AATACA	3
AATAGA	3

Table 1: Motif distribution

The next step was to create a negative dataset consisting of non-functional motives to determine the specificity. While it is possible to search the genome for true negative motives in any region that is not a 3' UTR, we instead decided to shuffle each sequence of the positive dataset maintaining the motif at its original position. The problem with the first approach is that we didn't know if the found matches were truly non-functional. They could have been part of a pseudogene or a not yet discovered transcript.

¹ftp://ftp.ncbi.nih.gov/genomes/H_sapiens/RNA/rna.gbk.gz. Version used from: 20.11.2016

3 Results

3.1 Coole ergebnisse für coole Menschen

3.2 Resultate, die die Welt verändern werden. So Great!

4 Conclusion/Discussion

Hello, here is some text without a meaning. This text should show what a printed text will look like at this place. If you read this text, you will get no information. Really? Is there no information? Is there a difference between this text and some nonsense like “Huardest gefburn”? Kjift – not at all! A blind text like this gives you information about the selected font, how the letters are written and an impression of the look. This text should contain all letters of the alphabet and it should be written in of the original language. There is no need for special content, but the length of words should match the language.

References

- [1] S. H. Bernhart, U. Muckstein, and I. L. Hofacker. RNA Accessibility in cubic time. *Algorithms Mol Biol*, 6(1):3, Mar 2011.
- [2] G. Brawerman. The Role of the poly(A) sequence in mammalian messenger RNA. *CRC Crit. Rev. Biochem.*, 10(1):1–38, 1981.
- [3] Y. Cheng, R. M. Miura, and B. Tian. Prediction of mRNA polyadenylation sites by support vector machine. *Bioinformatics*, 22(19):2320–2325, Oct 2006.
- [4] M. EDMONDS and R. ABRAMS. Polynucleotide biosynthesis: formation of a sequence of adenylate units from adenosine triphosphate by an enzyme from thymus nuclei. *J. Biol. Chem.*, 235:1142–1149, Apr 1960.
- [5] M. Edmonds, M. H. Vaughan, and H. Nakazato. Polyadenylic acid sequences in the heterogeneous nuclear RNA and rapidly-labeled polyribosomal RNA of HeLa cells: possible evidence for a precursor relationship. *Proc. Natl. Acad. Sci. U.S.A.*, 68(6):1336–1340, Jun 1971.
- [6] R. Elkon, A. P. Ugalde, and R. Agami. Alternative cleavage and polyadenylation: extent, regulation and function. *Nat. Rev. Genet.*, 14(7):496–506, Jul 2013.
- [7] J. H. Graber, G. D. McAllister, and T. F. Smith. Probabilistic prediction of *Saccharomyces cerevisiae* mRNA 3'-processing sites. *Nucleic Acids Res.*, 30(8):1851–1858, Apr 2002.
- [8] A. Hajarnavis, I. Korf, and R. Durbin. A probabilistic model of 3' end formation in *Caenorhabditis elegans*. *Nucleic Acids Res.*, 32(11):3392–3399, 2004.
- [9] M. Kalkatawi, F. Rangkuti, M. Schramm, B. R. Jankovic, A. Kamau, R. Chowdhary, J. A. Archer, and V. B. Bajic. Dragon PolyA Spotter: predictor of poly(A) motifs within human genomic DNA sequences. *Bioinformatics*, 29(11):1484, Jun 2013.
- [10] M. Kamasawa and J. Horiuchi. Prediction of non-canonical polyadenylation signals in human genomic sequences based on a novel algorithm using a fuzzy membership function. *J. Biosci. Bioeng.*, 107(5):569–578, May 2009.
- [11] M. Legendre and D. Gautheret. Sequence determinants in human polyadenylation site selection. *BMC Genomics*, 4(1):7, Feb 2003.
- [12] H. Liu, H. Han, J. Li, and L. Wong. An in-silico method for prediction of polyadenylation signals in human sequences. *Genome Inform*, 14:84–93, 2003.

- [13] R. Lorenz, S. H. Bernhart, C. Honer Zu Siederdissen, H. Tafer, C. Flamm, P. F. Stadler, and I. L. Hofacker. ViennaRNA Package 2.0. *Algorithms Mol Biol*, 6:26, Nov 2011.
- [14] S. Matis, Y. Xu, M. Shah, X. Guan, J. R. Einstein, R. Mural, and E. Uberbacher. Detection of RNA polymerase II promoters and polyadenylation sites in human DNA sequence. *Comput. Chem.*, 20(1): 135–140, Mar 1996.
- [15] J. S. McCaskill. The equilibrium partition function and base pair binding probabilities for RNA secondary structure. *Biopolymers*, 29(6-7): 1105–1119, 1990.
- [16] A. A. Salamov and V. V. Solovyev. Recognition of 3'-processing sites of human mRNA precursors. *Comput. Appl. Biosci.*, 13(1):23–28, Feb 1997.
- [17] R. Sandberg, J. R. Neilson, A. Sarma, P. A. Sharp, and C. B. Burge. Proliferating cells express mRNAs with shortened 3' untranslated regions and fewer microRNA target sites. *Science*, 320(5883):1643–1647, Jun 2008.
- [18] Y. Shen, G. Ji, B. J. Haas, X. Wu, J. Zheng, G. J. Reese, and Q. Q. Li. Genome level analysis of rice mRNA 3'-end processing signals and alternative polyadenylation. *Nucleic Acids Res.*, 36(9):3150–3161, May 2008.
- [19] J. E. Tabaska and M. Q. Zhang. Detection of polyadenylation signals in human DNA sequences. *Gene*, 231(1-2):77–86, Apr 1999.
- [20] M. Zuker and P. Stiegler. Optimal computer folding of large RNA sequences using thermodynamics and auxiliary information. *Nucleic Acids Res.*, 9(1):133–148, Jan 1981.